

This article was downloaded by:

On: 25 January 2011

Access details: *Access Details: Free Access*

Publisher *Taylor & Francis*

Informa Ltd Registered in England and Wales Registered Number: 1072954 Registered office: Mortimer House, 37-41 Mortimer Street, London W1T 3JH, UK



## Liquid Crystals

Publication details, including instructions for authors and subscription information:

<http://www.informaworld.com/smpp/title~content=t713926090>

### Elastic constant anisotropy and disclination interaction in nematic polymers I. Apparent variation in anisotropy

Wenhui Song<sup>a</sup>; Xudong Fan<sup>a</sup>; Alan H. Windle Corresponding author<sup>a</sup>; Shouxi Chen<sup>b</sup>; Renyuan Qian<sup>b</sup>

<sup>a</sup> Department of Materials Science and Metallurgy, Cambridge University, Cambridge CB2 3QZ, UK <sup>b</sup> Institute of Chemistry, Chinese Academy of Sciences, Beijing 100080, PR China

Online publication date: 19 May 2010

**To cite this Article** Song, Wenhui , Fan, Xudong , Windle Corresponding author, Alan H. , Chen, Shouxi and Qian, Renyuan(2003) 'Elastic constant anisotropy and disclination interaction in nematic polymers I. Apparent variation in anisotropy', *Liquid Crystals*, 30: 7, 765 – 774

**To link to this Article:** DOI: 10.1080/026782903100011469

**URL:** <http://dx.doi.org/10.1080/026782903100011469>

PLEASE SCROLL DOWN FOR ARTICLE

Full terms and conditions of use: <http://www.informaworld.com/terms-and-conditions-of-access.pdf>

This article may be used for research, teaching and private study purposes. Any substantial or systematic reproduction, re-distribution, re-selling, loan or sub-licensing, systematic supply or distribution in any form to anyone is expressly forbidden.

The publisher does not give any warranty express or implied or make any representation that the contents will be complete or accurate or up to date. The accuracy of any instructions, formulae and drug doses should be independently verified with primary sources. The publisher shall not be liable for any loss, actions, claims, proceedings, demand or costs or damages whatsoever or howsoever caused arising directly or indirectly in connection with or arising out of the use of this material.

# Elastic constant anisotropy and disclination interaction in nematic polymers

## I. Apparent variation in anisotropy

WENHUI SONG, XUDONG FAN, ALAN H. WINDLE\*

Department of Materials Science and Metallurgy, Cambridge University,  
Pembroke Street, Cambridge CB2 3QZ, UK

SHOUXI CHEN and RENYUAN QIAN

Institute of Chemistry, Chinese Academy of Sciences, Beijing 100080, PR China

(Received 22 August 2002; accepted 10 February 2003)

This work presents the effect of elastic anisotropy and disclination interaction on wedge disclinations in the nematic phase of thermotropic polymers, by combining experimental measurements, (this paper part I), with numerical simulation (part II [1]). In part I, the decoration provided by spontaneous banded texture gives much information about the defect structure of polymeric nematics. Working with a semi-rigid polyester, the optical images of  $+1/2$  disclinations revealed by banding enable the distortion to be determined as a function of polar coordinates from the cores. Continuum theory allows the apparent elastic anisotropy,  $\epsilon_a$ , of bend and splay constants of the copolyester to be determined from the distortion measurement. The values of  $\epsilon_a$  are seen to vary greatly in the range  $-1$  to  $+1$  between different  $+1/2$  disclinations in the same sample. The statistics of the measurement indicate that the distribution of the values of  $\epsilon_a$  is random. The implication of these observations is that the curvature of wedge disclinations is affected not only by the elastic anisotropy of the material, but also by other factors. The possible reasons are discussed: the interaction of neighbouring disclinations has been numerically analysed to be the predominant factor in [1]. This work also implies that values of the intrinsic elastic anisotropy obtained by measuring the distortion of individual wedge disclinations must be viewed with some circumspection.

### 1. Introduction

Although the defects and optical textures of liquid crystalline polymers (LCPs) are found also for low molecular mass liquid crystals (LMMLCs), the high molecular mass, chain flexibility and polydispersity of the polymers do have a strong influence on optical and rheological properties, and hence result in some unique features. The high viscosity and correspondingly long relaxation times of LCPs provide more opportunities to study the defects and their interactions in a metastable state. Another advantage is that the mesophase may be quenched to the glassy state. One of the well known phenomena of LCPs is the occurrence of band texture under certain conditions. This texture can be observed under polarized light during the relaxation of oriented nematic or cholesteric phases [2, 3]. On the other hand, without previous orientational treatment, a spontaneous

band texture is apparent during the solidification of some nematic melts of polymers after annealing [4, 5]. Fischer *et al.* [6] have proposed a buckling mechanism to explain the formation of band textures, both with and without shearing. As the bands are normal to the director field, when measured on a scale larger than their spacing, they can be used to decorate, and thus understand the preferred orientation within a larger scale texture, such as the director field around disclinations [7, 8].

Another significant feature that differentiates liquid crystalline polymers from low molecular mass liquid crystals is generally believed to be the pronounced elastic anisotropy. The study of anisotropy in the elastic properties of LCPs becomes fundamentally important for the understanding of the intrinsic relationship between molecular structure, microstructure and anisotropic mechanical properties, and for the guiding of the development of related theory. The anisotropy in splay and bend elastic constants considered by

\*Author for correspondence;  
e-mail: ahwl@cam.ac.uk

Dzytaloshinskii [9] and Nehring and Saupe [10] in the low molecular mass liquid crystal system, has been defined as:

$$\varepsilon = \frac{k_{11} - k_{33}}{k_{11} + k_{33}} \quad (1)$$

where  $k_{11}$  and  $k_{33}$  represent the curvature elastic constants for splay and bend deformations of the director  $\mathbf{n}$ , respectively.

Further theoretical investigation on the effect of elastic anisotropy was undertaken later by Ranganath [11] in great detail. His results predicted that the elastic anisotropy would alter the energies and the patterns of individual defects as well as their interaction. The distortion around the singularity of  $+1/2$  disclination depended dramatically on the elastic anisotropy, while the structure of  $-1/2$  disclination depended only weakly on it. The elastic constants for low molecular mass liquid crystals could be directly measured by using Fréedericksz transitions or by determining the amplitude of thermal fluctuations by light scattering [12]. In many cases, the three Frank elastic constants are of the same order of magnitude in small molecule liquid crystals, so the approximation  $k_{11} = k_{22} = k_{33}$  is valid in most circumstances. This equi-constant assumption is not, however, reasonable in long chain liquid crystalline systems. Owing to the experimental difficulties involved, the elastic constants of only a few LCPs have been estimated or measured to date, e.g. for thermotropic LCPs [13–18]. Frank [19] first proposed that the bend-to-splay elastic constant ratio would be obtained by measuring a non-uniform rotation of the extinction brushes emanating from a singularity with uniform rotation of polarizer and analyser. However, this method has not been performed because of the difficulty of the precise measurement. Hudson and Thomas [15, 16] developed a lamellar decoration technique under transmission electron microscopy (TEM), through which the bend-to-splay elastic constant ratios of LCPs were determined by directly measuring the relative amounts of distortion produced by a wedge disclination at a resolution of  $50 \sim 100$  nm. The elastic anisotropies of rigid and semiflexible LCPs as a function of radius from the disclination cores were compared with each other. A similar method [20] was applied to measure the elastic anisotropy of a lyotropic polymer.

Meanwhile, the theoretical prediction of elastic constants in liquid crystalline polymers has been developed. Meyer [21] and Odijk [22] deduced analytical expressions for the three elastic constants, depending only on the chain length, the persistence length and the molecular diameter in liquid crystalline polymers. On the basis of their equations, the Frank elastic constants could be determined from the persistence length itself

obtained by using a Monte Carlo molecular-scale modeling [23]. A hierarchical approach [24] to computer modelling of liquid crystalline polymers was developed to describe their structure and behaviour. Lattice models considering the case of unequal Frank constants were built to predict the microstructure of LCPs, to simulate the evolution of defects, and to simulate their response to complex boundary conditions and applied fields [25, 26].

The work reported in this paper is based on the experimental measurement of distortion fields around wedge disclinations in a liquid crystalline polymer. The work involves image analysis of the director field decorated by spontaneous band texture to obtain information about the distortion around the core of wedge disclinations. The values of apparent elastic constant anisotropy have been measured for a large number of wedge disclinations as a function of radial distance from  $+1/2$  cores. The values obtained for the anisotropy vary randomly, over a wide range, from disclination to disclination. In the companion paper [1], a tensor lattice model has been applied to reveal the reason for this.

## 2. Determination of elastic anisotropy by optical band texture

Previous work [4, 7] presented the formation and decoration application of the spontaneous band texture in a thermotropic main chain aromatic copolymer with a flexible hexamethylene spacer which we term Cl-6:

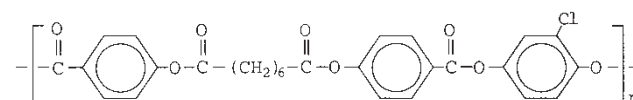


Figure 1(a) shows the unoriented band texture of a Cl-6 thin film (about  $10 \mu\text{m}$  in thickness) under a polarizing light microscope. The long axes of the bands were normal to the local mesogen director orientation; thus the director field was revealed in the optical texture by bands which were around  $1 \mu\text{m}$  wide [4, 7, 8]. The prerequisite of this method is that the scale of the microstructure to be decorated is significantly larger than the spacing of the bands. It is therefore useful for structures with comparatively low disclination densities. For instance, the disclination density in figure 1(a) is about  $3 \times 10^3 \text{ mm}^{-2}$  (considered as two-dimensional situation because of wedge disclinations), where the distance between the majority of disclinations is in the range  $7\text{--}18 \mu\text{m}$ . Furthermore, using a method similar to that proposed by Hudson *et al.* [15] for measuring the distortion of lamellae, it is possible to determine the orientation of the band around the disclination in order to calculate the elastic anisotropy of the LCP.

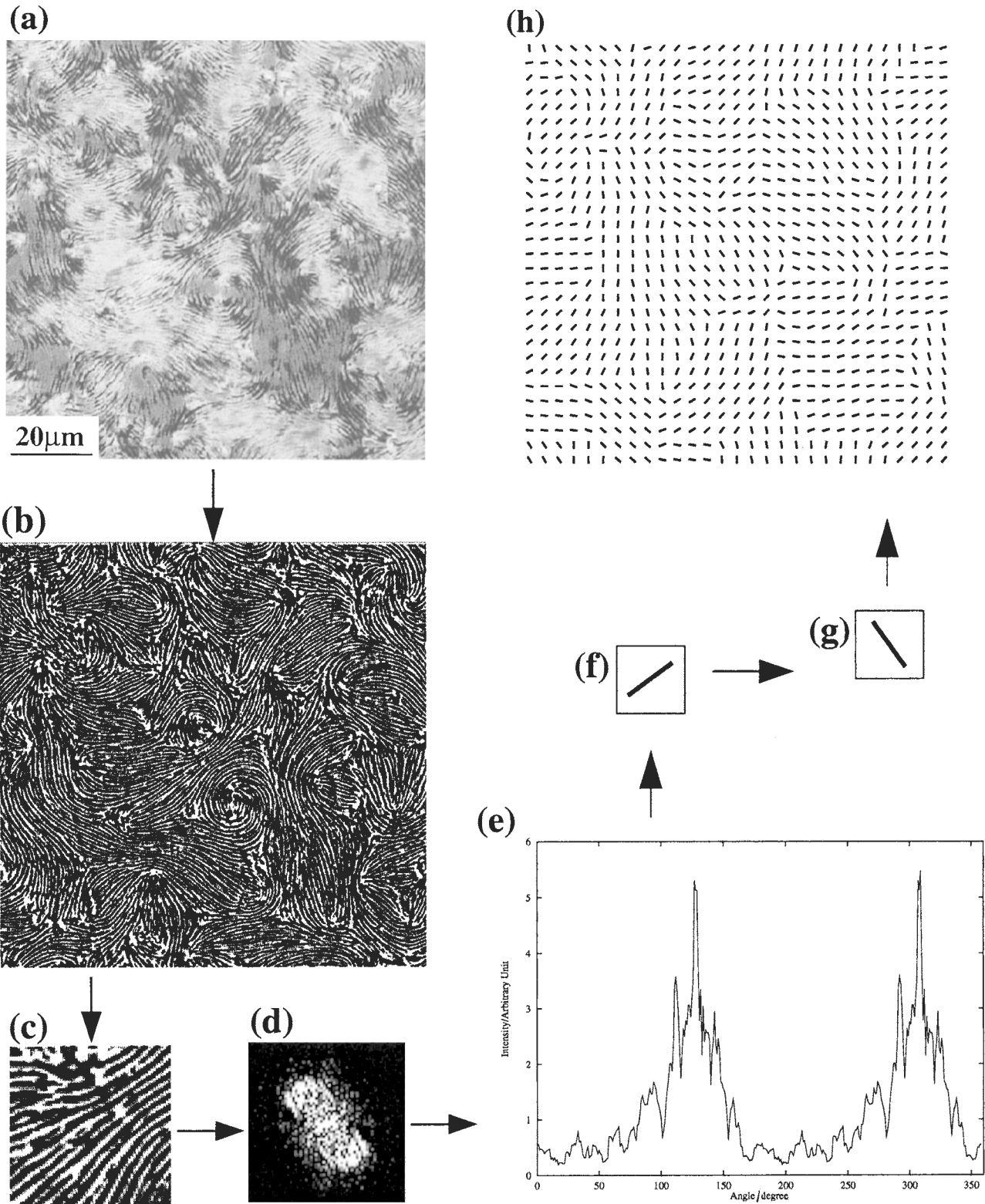


Figure 1. (a) The spontaneous band texture in a quenched film of Cl-6 copolyester under the polarizing optical microscope between two polarizers; (b) A digitally enhanced image of the spontaneous band texture; (c) A selected unit image; (d) The power spectrum obtained by fast Fourier transform; (e) The radial integration of power spectrum as a function of angle; (f) The direction of the band long axis; (g) The average orientation of molecular director in the unit image obtained from the angular distribution function; (h) The map of the director field from (a).

### 2.1. Image processing and director mapping

In order to obtain a description of the director field from the experimentally observed optical band texture, a digital image processing algorithm was applied. The image analysis was adapted from the method of analysing the packing morphology of carbon nanotubes [27] using the *image* analysis software, *xview*.

The analysis procedure is illustrated in figure 1. Firstly, an optical picture of spontaneous band texture, figure 1 (a), was digitized using a scanner to give a grey scale image. Figure 1 (a) is a micrograph of the spontaneous band texture at a relatively low magnification ( $150 \times 150 \mu\text{m}^2$ ). The image was then processed by filtering out both high and low frequencies to enhance the band texture. The very low frequency background was removed by a low pass filter, and the very high frequency by local averaging, figure 1 (b). In order to obtain the local director, a small unit image was extracted, figure 1 (c), and the power spectrum obtained by the fast Fourier transform method, figure 1 (d). The power spectrum is space-independent and hence the angular distribution of the intensity represents the angular distribution of the orientation of the bands, figure 1 (e). The average band orientation in the extracted unit image can be defined as the angle at which this distribution is a maximum, figure 1 (f). Finally, the real average direction of the molecular director in this unit image was given as that perpendicular to the average band orientation, figure 1 (g). A discrete map of the orientation distribution of the molecular director was generated by systematically repeating the above procedure from figures 1 (c) to (g), as shown in figure 1 (h).

Measurements of the orientation of the director were obtained at points corresponding to the location of the centre of each unit image. The size of unit image and the step between the neighbouring unit images were varied, and determine the resolution of the discrete director map. Every disclination image ( $29 \times 29 \mu\text{m}^2$ ) for the measurement in the following sections was converted into a signal with a size of  $450 \times 450 \text{ pixel}^2$ . A  $64 \times 64 \text{ pixel}^2$  (about  $4 \times 4 \mu\text{m}^2$ ) unit image and 16 or 8 pixel (about 1 or  $0.5 \mu\text{m}^2$ ) steps were sufficiently fine to resolve the optical image in this image processing. The step reached the resolution of the optical image because the spacing of the band was about  $1 \mu\text{m}$ .

### 2.2. Method of measurement

In a thin film, the defects are wedge disclinations around which the directors may be confined to lie in the plane of the film. In this case, the disclination lines are normal to the surface and only splay and bend distortions are likely. In figure 2 (a), the core of an isolated

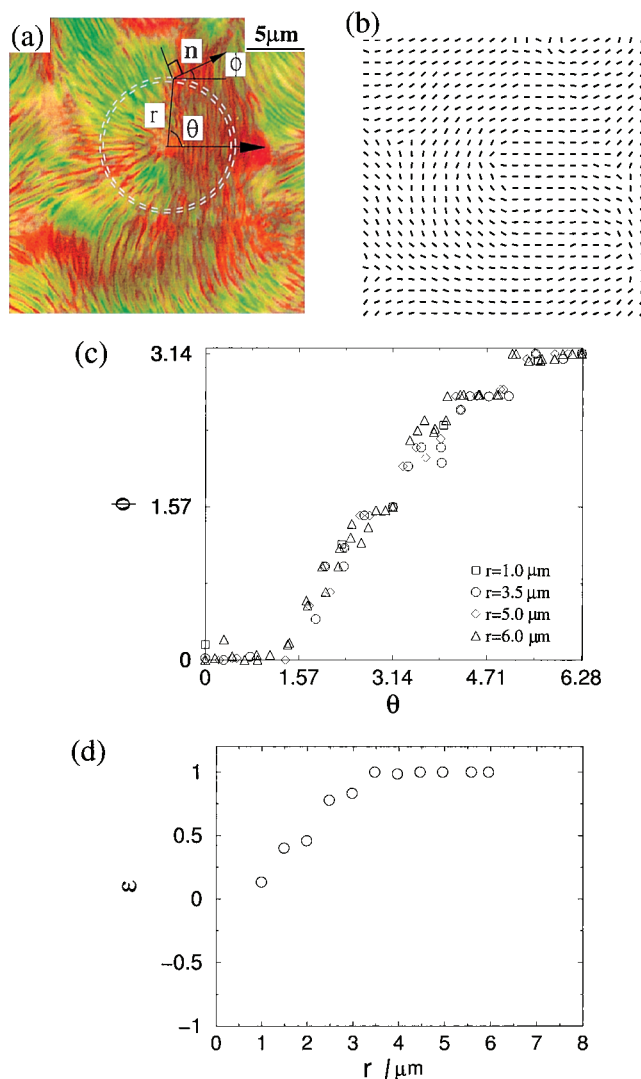


Figure 2. (a) An isolated  $+1/2$  disclination of Cl-6 copolyester revealed by the band texture. The director angle  $\phi$  describes the orientation of the molecular director along a polar line making an angle  $\theta$  to an appropriate axis at a distance  $r$  from the singularity core. (b) The corresponding director field from (a). (c) The  $\phi(\theta)$  data measured from the disclination (a) at  $r = 1.0, 3.5, 5.0$  and  $6.0 \mu\text{m}$  are obtained from the director field (b). (d) The values of  $\varepsilon$  at different radius  $r$ ,  $\varepsilon(r)$ .

disclination is chosen as an origin in polar coordinates. The director angle  $\phi$  describes the orientation of the molecular director along a polar line making an angle  $\theta$  with an appropriate axis at a distance  $r$  from the origin. According to continuum theory, the distortional free energy density,  $f$ , around an isolated disclination is described in polar coordinates as [28]:

$$f = \left( \frac{k}{2r^2} \right) \left( \frac{\partial \phi}{\partial \theta} \right)^2 [1 + \varepsilon \cos 2(\phi - \theta)] \quad (2)$$

where  $k = 1/2(k_{11} + k_{33})$ . A second order non-linear differential equation, which describes the relation between  $\phi$  and  $\theta$  in the most probable director configuration, can be described by minimizing the total free energy with respect to the two-dimensional director field [28]:

$$\begin{aligned} \varepsilon \left[ \frac{\partial^2 \phi}{\partial \theta^2} \cos 2(\phi - \theta) + \frac{\partial \phi}{\partial \theta} \left( 2 - \frac{\partial \phi}{\partial \theta} \right) \sin 2(\phi - \theta) \right] \\ = - \frac{\partial^2 \phi}{\partial \theta^2}. \end{aligned} \quad (3)$$

For small values of  $|\varepsilon|$ , a first order perturbation expansion given by Nehring and Saupe [10] can be used to calculate the value of  $\varepsilon$  directly.

$$\phi = s\theta + c + \varepsilon \left\{ \frac{s(2-s)}{4(s-1)^2} \sin[2(\theta(s-1) + c)] + c' \right\} \quad (4)$$

where  $s$  is the topological strength of a disclination and  $c$  and  $c'$  are constants which influence the orientation of the disclination. Wang *et al.* [20] claimed that equation (4) can be used only within  $-0.667 < \varepsilon < 0.667$ , but a significant deviation appeared when  $|\varepsilon| > 0.4$ . However, the values of  $\varepsilon$  for main chain thermotropic LCPs are most likely greater than 0.4, as reported in the literature [13, 18]. In this case, elastic constant anisotropy should be calculated from the numerical solution of equation (3) by fitting the experimental data as shown in figure 2(c).

The distortion data  $\phi(\theta)$  can be obtained from the director field mapped by the above-described image analysis. The origin is defined once the disclination core position has been identified. Hence the director field data  $\phi(\theta)$  at radius  $r$  can be determined. As shown in figure 2(a), all data points inside the ring between radius  $r$  and  $r + \Delta r$  are included in the data  $\phi(\theta)$  ( $\Delta r = \text{step} - 0.1$ ;  $\Delta r \approx 1 \mu\text{m}$  if  $\text{step} = 16$  pixel and  $\Delta r \approx 0.5 \mu\text{m}$  if  $\text{step} = 8$  pixel). The number of data points increases with the radius. Figure 2(c) gives examples of  $\phi(\theta)$  data measured from the disclination at distance  $r = 1.0, 3.5, 5.0$  and  $6.9 \mu\text{m}$ . The first derivative  $\partial\phi/\partial\theta$  and the second derivative  $\partial^2\phi/\partial\theta^2$  can be approximated using central finite difference from the  $\phi(\theta)$  data. The elastic anisotropy  $\varepsilon$  at different radius  $r$ ,  $\varepsilon(r)$ , is determined by a least-square fit to equation (3) and shown in figure 2(d).

### 3. Elastic anisotropy measured from a disclination

Disclinations of topological strength  $+1/2$  were used in this measurement, as its distortion was predicted to depend greatly on elastic anisotropy [9, 11, 15]. Theoretically, elastic anisotropy is independent of the radius. In the measurement, for the majorities of  $+1/2$  disclinations closely surrounded by neighbours the

values of  $\varepsilon$  were rarely constant as the radius increased, and deviated further when the radius approached neighbouring disclinations. However, the impact of multiple disclination interactions is a complicating factor. Only for some  $+1/2$  disclinations with distant neighbouring disclinations (separation distance larger than  $10 \mu\text{m}$ ), the function  $\varepsilon(r)$  levelled off at around one when radii were greater than about  $2.5 \mu\text{m}$ , as shown in figure 2(d). Therefore, only the  $+1/2$  disclinations with a distance greater than  $10 \mu\text{m}$  to its nearest neighbour were chosen for measurement.

The Frank theory is not suitable for describing the core structure of a disclination, since the energy density becomes infinite when  $r$  approaches zero. On the other hand, the deformation energy of the core is, in general, considered to be smaller than the gain in free energy due to the orientational order of a corresponding volume. The effect of the core is confined to a radius less than the wavelength of light and is therefore beyond the resolution of an optical microscope.

The values of  $\varepsilon$  at radii less than about  $2.5 \mu\text{m}$  would have been less reliable, see figure 2(d). There are fewer data points available when approaching the core of the defect. For instance, only four data points of  $\phi(\theta)$  are measured at a radius of  $1 \mu\text{m}$  in figure 2(c). Therefore, the  $\phi(\theta)$  data are insufficient to describe the actual trajectory change of the bands when approaching the core of the defect. In many other cases of  $+1/2$  disclinations (measured in the next section), the values of  $\varepsilon$  may decrease or increase with the radii near the cores [see figure 4(b)]. However, the core effect is negligible in the optical measurement as lower values are not possible.

In the following measurements of other disclinations of  $+1/2$ , the value of the elastic anisotropy measured from one disclination is defined as a mean of values of  $\varepsilon$  in the range of radii larger than  $2.5 \mu\text{m}$  and less than a half of the distance,  $d$ , between the nearest neighbouring disclinations. For the disclination in figure 2, the mean of  $\varepsilon$  is 0.99 measured in a range of radii from 2.5 to  $8.0 \mu\text{m}$ .

### 4. Variations of the elastic anisotropy

As mentioned already, this measurement was supposed to be a method for measuring the splay-bend elastic anisotropy of LCPs. However, after measuring a number of  $+1/2$  disclinations, it became clear that the issue was not straightforward. Figures 3 and 4 show the measurements from four disclinations in one specimen. It can be seen from figure 4(b) that the values of the elastic anisotropy measured from these selected disclinations change dramatically from  $-1$  to  $+1$ . In figure 3(a), two neighbouring  $+1/2$  disclinations are revealed by bands in two extreme patterns, one showing a bending 'archway' (a1) and another a completely

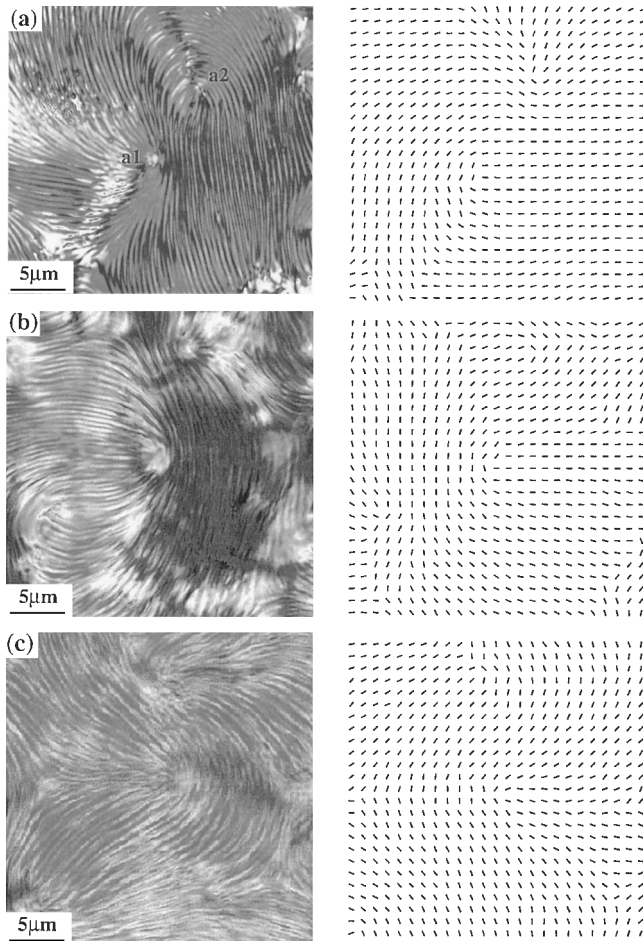


Figure 3. Four  $+1/2$  disclinations of Cl-6 copolyester showing different distortions revealed by the orientation of bands and the corresponding director fields obtained by image analysis. In (a), there are two neighbouring  $+1/2$  disclinations showing two extreme structures, one is mostly bend ('archway') (a1) and the other mostly splay ('sunrise') (a2). The distortions around disclinations (b) and (c) show both bend and splay, however the bend distortion is in the greater proportion in (b) while splay is in (c).

'sunrise' splay structure (a2). Consequently, the mean values of the elastic anisotropy  $\varepsilon$  measured from these two disclinations show opposite signs, *i.e.* for disclination (a1),  $\varepsilon=1.00$ , and for disclination (a2),  $\varepsilon=-0.98$ . Mean values of  $\varepsilon$  within the range  $-1$  and  $+1$  also appear for the disclinations shown in figures 3(b) and 3(c), specifically  $0.37$  and  $-0.56$  respectively. According to the definition of the splay-bend anisotropy,  $\varepsilon=(k_{11}-k_{33})/(k_{11}+k_{33})$ , the measured values of  $\varepsilon$  imply that the bend constant could be much greater than the splay constant measured from one  $+1/2$  disclination and much less than that measured from another in this material. Obviously, this implication makes no sense. The values of the elastic anisotropy obtained by

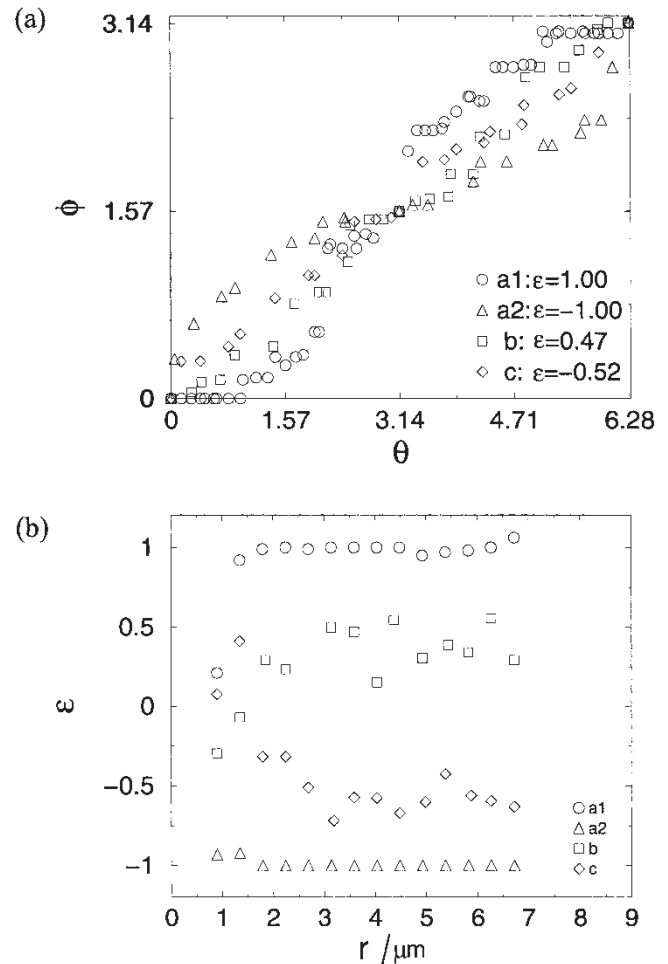


Figure 4. The measurements from the four  $+1/2$  disclinations of Cl-6 copolyester shown in figure 3. (a) The  $\phi(\theta)$  data measured from these four disclinations at the same radius  $r=3.6\mu\text{m}$ . (b) The results of  $\varepsilon(r)$  measured from these four disclinations.

measuring distortions around a single  $+1/2$  disclination do not appear to represent intrinsic elastic anisotropy for the LCP, and are therefore termed as *apparent* elastic anisotropy,  $\varepsilon_a$ .

A large number of repeat measurements have been carried out in order to determine the distribution of the *apparent* elastic anisotropy and to understand the change of distortions in different disclinations of strength  $s=+1/2$  for the Cl-6 polymer. The advantage of this measurement is that a large number of disclinations revealed by the band texture under the polarizing microscope are available. Figure 5 shows the distribution of the values of  $\varepsilon_a$  measured from sixty disclinations of strength  $s=+1/2$ . The histogram is constructed with all the values of  $\varepsilon_a$  rounded up or down to the first decimal place. This distribution is not easily characterized or interpreted. This figure shows

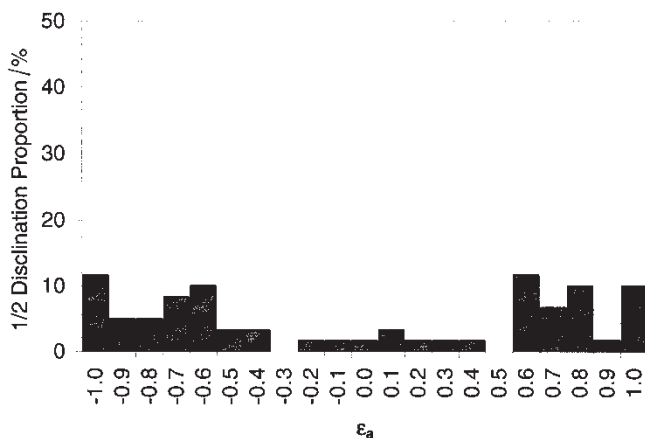


Figure 5. The distribution of the mean values of  $\epsilon_a$  measured from sixty disclinations of  $s = +1/2$  in nematics of Cl-6 copolyester.

that the probabilities of each value of  $\epsilon_a$  ( $-1 \leq \epsilon \leq 1$ ) is not greater than 15%, *i.e.* there is no value of  $\epsilon_a$  which is statistically dominant. Therefore, the distortions around the defect tend either to bend or to splay, or show some intermediate situation of both bend and splay. In fact, it can be seen that the band orientation around the cores of  $+1/2$  disclinations changes significantly from figure 3(a) to figure 3(c) in one specimen. Furthermore, a number of disclinations reach the limits  $\pm 1$ , and the corresponding director field is either completely free of splaying distortions ( $\epsilon_a = +1$ ), an ‘archway’ structure, [figure 3(a1)], or free of the bend distortion ( $\epsilon_a = -1$ ), a ‘sunrise’ structure [figure 3(a2)].

Obviously, such pronounced variations in the elastic anisotropy for one kind of material seem unreasonable. According to theoretical studies for the unequal elastic constant case [10, 11], the distortion of disclinations of strength  $s = +1/2$  is only a function of elastic anisotropy  $\epsilon$ . In other words, the distortion in disclinations of the same topology ( $+1/2$ ) could vary from one liquid crystal to another if their elastic anisotropies differ. However, for every liquid crystalline material, its elastic constant anisotropy  $\epsilon$  should be a constant which takes into account the energy of curvature and patterns of the director field of that particular material. Therefore,  $+1/2$  disclinations should exhibit just one distortion pattern for a given material. The difference between the theoretical prediction and our measurements means that the changes of curvature in wedge disclinations of strength  $+1/2$  are not exclusively determined by elastic splay–bend anisotropy.

In addition, the wide distribution of  $\epsilon_a$  in figure 5 seems to give a hint that the intrinsic elastic anisotropy for the semi-rigid Cl-6 copolyester may be around zero (the mean of  $\epsilon_a$  is  $-0.08$ ), if compared with the values

of  $\epsilon_a$  measured from the simulated disclinations using equal and unequal elastic constants in [1]. It would appear that the apparent elastic anisotropy varies between  $-1$  and  $+1$  in the case of  $\epsilon = 0$ . There will be further discussion and evidence of this in [1].

## 5. Discussion on the variations of elastic anisotropy

### 5.1. Errors of the measurement

The possible sources of error in the determination of elastic anisotropy by measuring the distortion around the disclination using the lamellar decoration method have been discussed extensively [15, 16]. Similarly, there are many factors which may introduce errors to the measured elastic anisotropy in the band decoration method, such as the resolution of the image, the determination of the position of the singularities, interactions with neighbouring disclinations and so on. Firstly, the optical band resolution of  $0.5 \sim 1 \mu\text{m}$  increases the error in determining the distortion of the disclination, compared with that of lamellae observed under a transmission electron microscope (the period of the lamellae is about  $50 \sim 100 \text{ nm}$  in the lamellar decoration method) [15]. Secondly, the effect of miscentring the origin on the disclination is obvious. In this measurement, the position of the disclination is determined from the discrete director field obtained from the image processing. One pixel in the centre of the symmetric director pattern is chosen as the origin of the disclination, and the error in miscentring can be less than or equal to the band spacing. On the other hand, compared with the lamellar structure, the continuous and distinct bands make it easy and accurate to measure the orientation of the director from the local power spectrum as it essentially gives rise to a strong peak corresponding to the band orientation in Fourier space; see figure 1(d) and 1(e). Therefore, the combined error introduced by this optical method of determination should be acceptable, and cannot cause such big differences in the value of  $\epsilon$  measured from different disclinations.

### 5.2. Effect of polydispersity of LCPs

The following discussion is on the characteristic features of the polymer that may contribute to the variations of  $\epsilon_a$  calculated from different  $+1/2$  disclinations. The polydispersity of a polymer would have an important influence on the elastic constants. Meyer [21] demonstrated that the splay constant increased with molecular weight for LCPs; the twist and bend constants, however, depended on the persistence length. The elastic constants can be expressed in simplified equations for main chain thermotropic polymers given by



Meyer [21] and Odijk [22].

$$k_{11} \approx \frac{kT}{D} \left( \frac{L}{D} \right) \quad (5)$$

$$k_{22} \approx \frac{kT}{D} \left( \frac{p}{D} \right)^{\frac{1}{2}} \quad (6)$$

$$k_{33} \approx \frac{kT}{D} \left( \frac{p}{D} \right) \quad (7)$$

where  $p$  is the persistence length of the chain,  $L$  the contour length of the chain,  $D$  the diameter of the molecules,  $k$  the Boltzmann constant and  $T$  is the temperature in Kelvin.

According to Meyer and Odijk's prediction, if the chains are sufficiently long, the persistence length reaches a limit which becomes independent of molecular mass, while the contour length increases with molecular mass, and hence so does the splay constant, without reaching a limiting value. Thus, for thermotropic main chain LCPs, the splay constant may be significantly larger than either the twist or the bend constants. The bend distortion is energetically favoured. It can be inferred that the splay–bend elastic anisotropy of a LCP should always be positive and also show a Gaussian distribution of values similar to the typical distribution of the molecular mass of polymers.

As a matter of fact, the histogram of  $\varepsilon_a$  in figure 5 shows that the distribution of  $\varepsilon_a$  is wide and undetermined. Only about a half number of  $+1/2$  defects appear in the bend distortion favoured, the others are splay favoured, and in some extreme cases, the bend distortion is even prohibited. A negative value of  $\varepsilon$  was also measured from one  $+1/2$  disclination in a semi-rigid LCP using lamellar decoration method [15, 16]. Thus, the effect of polydispersity of the polymer may not be directly correlated with the variation of the apparent elastic anisotropy, perhaps at least for semi-rigid LCPs. De Gennes [29] and Khokhlov and Semenov [30] proposed that a hairpin bend could occur in a semi-rigid chain consisting of mesogens jointed by flexible spacers. The splay elastic constant of LCPs in the nematic state could be strongly influenced by hairpins. The hairpins could act in similar fashion to chain ends and lower the effective splay constant. The fact that the measured apparent anisotropy averaged to give a value  $-0.08$ . *i.e.* close to zero, suggests that there is no intrinsic anisotropy to produce a bias. It seems reasonable to suggest that this indicates an intrinsic anisotropy near to zero, as the polymer used contains flexible spacers and thus hairpins may reduce the otherwise high value expected for the splay constant.

Therefore, we now need to think in more detail about the real meaning of the measured values of the *apparent* elastic anisotropy  $\varepsilon_a$  and the relationship

between intrinsic elastic anisotropy and polydispersity in the LCPs. However, more theoretical and experimental work needs to be performed, and in particular on the second issue. The obvious disagreement also raises questions about the measurement method. The pronounced change of  $\varepsilon_a$  in the measurement may be due to the inapplicability of the theory rather than the real change of the elastic constants in the materials.

### 5.3. Effect of disclination interaction

In the continuum theory, the structure of a single disclination is deduced on the assumption of minimum elastic free energy. Therefore, the disclinations measured should ideally be isolated ones, and has been calculated in [1]. In reality, in polymers a state of ultimate thermodynamic stability is hardly ever attained, so the nematic state of the material does not meet the condition of being in a minimum total elastic free energy. It is rare to observe a purely isolated disclination in a polymeric mesophase. Even isolated pairs ( $+1/2$ ,  $-1/2$ ) are rare: each defect is surrounded by a host of other defects, some with positive and some with negative signs. Therefore, defect interactions may play an important role on defect structure.

To observe spontaneous bands, it is necessary to anneal the thermotropic sample at a relatively high temperature for about 10 to 20 min in the nematic phase. During the nematic annealing, the disclinations approach each other and annihilate to minimize their total elastic free energy. Eventually, the density of disclinations only decreases to a certain degree ( $10^3 \text{ mm}^{-2}$  for Cl-6 copolyester) because of the high viscosity of the sample melt and surface anchoring. In all disclinations measured, the distances to the nearest neighbouring disclinations are greater than  $10 \mu\text{m}$ , but nevertheless may have an effect as the resolution of the method is of the order of  $1 \mu\text{m}$ . Thus, it should be pointed out that the values measured from the distortions of any individual disclination are probably not good indications of the average material elastic anisotropy. The neighbouring defect interaction cannot be neglected. The wide distribution of the values of the apparent elastic anisotropy (as shown in figure 5) may just reflect the complex effect of the disclination interaction, resulting from a wide variety of patterns of disclination clusters in the real nematic system. It is nevertheless intriguing that the distortion obtained is largely independent of  $r$  as indicated by the plateau of figure 4(b).

Finally, it is interesting that some defect separation is observed, as shown in figure 6, which may provide some clues of the formation of  $+1/2$  disclinations with extreme patterns, such as 'sunrise'. Apparently, the almost con-

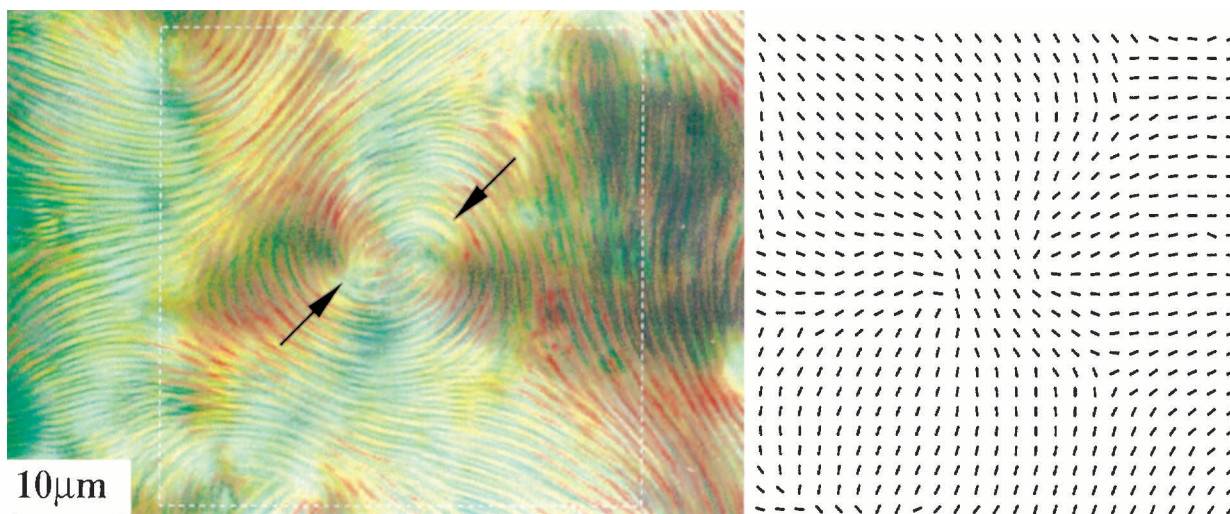


Figure 6. The separation of a radial integer disclination ( $s = +1$ ). As a result, the corresponding director trajectories show two close 'sunrise'  $+1/2$  disclinations.

centric band around a centre in figure 6 could be seen as a radial disclination ( $s = +1$ ,  $c = 0$ ). In fact, the corresponding director field obtained by the image analysis shows that there are two  $+1/2$  disclinations showing predominant splay 'sunrise', which would be easily associated with a split of an integer disclination ( $s = +1$ ,  $c = 0$ ) in the centre area. This image illustrates that the separated  $+1$  disclinations could be one of the sources resulting in the extreme curvature strain of  $+1/2$  disclinations. This provides evidence that various distortions of  $+1/2$  disclinations may exist and are strongly influenced by their local environment.

## 6. Conclusions

The distribution of the apparent elastic anisotropy measured optically from disclinations forming a texture is broad. The application of an optical method for determining distortion anisotropy of resolution of the order of  $1 \mu\text{m}$ , to a  $+1/2$  wedge disclination in an array where the mean spacing is a few  $10\text{s of } \mu\text{m}$ , gives a value of the distortion which appears to be determined more by the director field of the neighbours than by any intrinsic anisotropy. It is worthy of note however that the anisotropy of a given  $+1/2$  disclination in a given environment does appear constant over a distance of several microns out from the core. In the following paper, a tensor lattice model has been applied to modelling the influence of disclination interaction on anisotropy of these director fields [1].

W. S. would like to acknowledge the support of an Overseas Research Student (ORS) Scholarship,

Cambridge Overseas Trust Scholarship and the Department of Materials Science and Metallurgy, University of Cambridge.

## References

- [1] SONG, W., TU, H., GOLDBECK-WOOD, G., and WINDLE, A. H., 2003, *Liq. Cryst.*
- [2] DOBB, M. G., JOHNSON, D., and SAVILLE, B. P., 1977, *J. Polym. Sci. Polym. Phys. Ed.*, **15**, 2201.
- [3] VINEY, C., DONALD, A., and WINDLE, A. H., 1983, *J. Mater. Sci.*, **18**, 1136.
- [4] CHEN, S., DU, C., JIN, Y., QIAN, R., and ZHOU, Q., 1990, *Mol. Cryst. Liq. Cryst.*, **188**, 197.
- [5] HOFF, M., KELLER, A., ODELL, J. A., and PERCEC, V., 1993, *Polymer*, **34**, 1800.
- [6] FISCHER, H., KELLER, A., and WINDLE, A. H., 1996, *J. non-Newtonian Fluid Mech.*, **67**, 241.
- [7] CHEN, S., SONG, W., JIN, Y., and QIAN, R., 1993, *Liq. Cryst.*, **15**, 247.
- [8] SONG, W., CHEN, S., JIN, Y., and QIAN, R., 1996, *Liq. Cryst.*, **19**, 549.
- [9] DZYTALOSHINSKII 1970, *Sov. Phys. JETP*, **31**, 773.
- [10] NEHRING, J., and SAUPE, A., 1972, *J. Chem. Soc. Faraday Trans. II*, **68**, 1.
- [11] RANGANATH, G. S., 1983, *Mol. Cryst. Liq. Cryst.*, **97**, 77.
- [12] CHANDRASEKHAR, S., 1992, *Liquid Crystals* (Cambridge: University Press).
- [13] ZHENG-MIN, S., and KLÉMAN, M., 1984, *Mol. Cryst. Liq. Cryst.*, **111**, 321.
- [14] SE, K., and BERRY, G. C., 1987, *Mol. Cryst. Liq. Cryst.*, **153**, 133.
- [15] HUDSON, S. E., and THOMAS, E. L., 1989, *Phys. Rev. Lett.*, **62**, 1993.
- [16] HUDSON, S. D., FLEMING, J. W., GHOLZ, E., and THOMAS, E. L., 1993, *Macromolecules*, **26**, 1270.
- [17] DING, D-K., and THOMAS, E. L., 1993, *Macromolecules*, **26**, 6531.

- [18] DE'NEVE, T., and KLÉMAN, M., 1995, *Liq. Cryst.*, **18**, 67.
- [19] FRANK, F. C., 1958, *Discuss. Faraday Soc.*, **25**, 19.
- [20] WANG, W., HASHIMOTO, T., LIESER, G., and WEGNER, G., 1994, *J. Polym. Phys.*, **32**, 2171.
- [21] MEYER, R. B., 1982, *Polymer Liquid Crystals*, edited by W. R. Krigbaum, A. Ciferri, and R. B. Meyer (New York: Academic Press), p.133.
- [22] ODIJK, T., 1986, *Liq. Cryst.*, **1**, 553.
- [23] BEDFORD, S. E., YU, K., and WINDLE, A. H., 1992, *J. Chem. Soc., Faraday Trans*, **88**, 1765.
- [24] HOBDELL, J. R., LAVINE, M. S., and WINDLE, A. H., 1996, *J. Comput. Aided mater Des.*, **3**, 359.
- [25] HOBDELL, J. R., and WINDLE, A. H., 1997, *Liq. Cryst.*, **23**, 157.
- [26] TU, H., GOLDBECK-WOOD, G., and WINDLE, A. H., 2001, *Phys. Rev. E*, **64**, 1704.
- [27] SHAFFER, M. S. P., FAN, X., and WINDLE, A. H., 1998, *Carbon*, **36**, 1603.
- [28] KINI, U. D., and RANGANATH, G. S., 1977, *Mol. Cryst. Liq. Cryst.*, **38**, 311.
- [29] DE GENNES, P. G., 1982, *Polymer Liquid Crystals*, edited by W. R. Krigbaum, A. Ciferri, and R. B. Meyer, (New York: Academic Press) p.133.
- [30] KHOKHLOV, A. R., and SEMENOV, A. N., 1982, *J. Phys.*, **A15**, 1361.